IOP Conf. Series: Materials Science and Engineering **418** (2018) 012046 doi:10.1088/1757-899X/418/1/012046

Application of Non-Uniform Stretch Flanging Theory to Edge-Crack-Prevention Product Design

R Tabata[1], J Nitta[1], S Yonemura[1], M Mizumura[1] and S Hiwatashi[1]

[1]Nippon Steel & Sumitomo Metal Corporation, 20-1 Shintomi, Futtsu, Chiba 293-8511, Japan

E-mail: tabata.e63.ryoh@jp.nssmc.com

Abstract. In order to quickly obtain an appropriate (semi-)product shape that prevents edge fracture in stretch flanging, the non-uniform stretch flanging theory proposed by Nagai was applied to the prediction of strain distribution observed in sheet metal forming of a product with a flat top and a concave wall. The strains calculated by the finite difference method along the flange edge are comparable to those obtained by finite element analysis. Furthermore, flange height h, corner radius R, and shape angle θ were selected as significant factors on circumferential strain ε_c along the flange edge. The investigation on the effect of those factors shows that ε_c increases as R decreases, h increases, and as θ increases. A further increase in θ, however, reduces the increasing rate of ε_c.

1. Introduction

The application ratio of high-strength steel sheets to automobiles has increased recently in order to achieve both weight reduction of the car body and improvement of crash safety [1]. By contrast, the lower formability of high-strength steel sheets compared to that of mild steels is a subject of concern regarding its further utilization. In particular, cracking of sheared surfaces during stretch flange forming, hereafter called "edge cracking," has been identified as the main aspect requiring improvement.

When automotive parts are designed, it is necessary to prevent edge cracks during press forming. Therefore, in order to design a part shape using an appropriate steel type such as DP steel and TRIP steel, the stretch-flangeability of the steel sheet must be evaluated. Because edge cracking is a phenomenon in which cracks are generated at the edge of the steel sheet, it is effective to calculate the strain distribution at the edge. The relationship between part shapes and strain distribution at the edge was reported by Nitta et al. [2]. They conducted experiments to investigate the influence of the contour shape of parts and flange height on stretch-flangeability and evaluated the strain distribution for each condition by finite element analysis (FEA). However, this study is not directly used for actual automobile designing. The evaluation techniques require many experiments and FEA, and it takes a lot of time to evaluate the stretch flangeability. Therefore, to minimize the escalation in work time, a simple and accurate method of evaluating stretch flangeability should be developed. Hiwatashi et al. evaluated the relationship between the part shapes and stretch flangeability by theoretical calculations [3]. They evaluated the strain at the flange edge using uniform deformation theory. However the

influence of the part shapes on the non-uniform strain distribution at the flange edge has not been sufficiently studied. In order to evaluate non-uniform deformation by theoretical calculations, it is necessary to consider in-plane shear deformation occurring in the flange. Nagai reported on non-uniform stretch flanging analysis considering in-plane shear deformation [4]. Nagai investigated the accuracy of calculation and proposed a technique to prevent edge cracking. However, the quantitative influence of part shapes on stretch flangeability has not been studied.

In this study, we derive a part shape that does not generate edge cracking by adding our contribution to previous investigations on the stretch flangeability. In order to reveal the quantitative influence of part shapes on the strain distribution at the flange edge, the characteristics and accuracy of the result calculated by Nagai's method were investigated [4]. From the results, a method of deriving the part shapes that does not generate edge cracking was developed.

2. Non-uniform deformation theory in stretch flanging analysis

The non-uniform stretch flanging analysis proposed by Nagai is outlined as follows [4]. Figure 1 shows a schematic figure of the shape change before and after deformation. It is assumed that the area element *PQRS* before the deformation becomes *PQ'R'S* after the deformation. As the assumption of flange deformation, the line segment *PS* on the bottom surface of the part does not deform, the length of *Q'R'* is the same as the length of *PS*, and *PQ'* is perpendicular to *PS*. Assuming that *PQ'*, *SR'* become *PQ*, *SR* before deformation respectively, angle ψ_0 formed by *PQ* and the normal *PS* is the amount generated by shearing deformation before and after flange deformation. In this paper ψ_0 is called the "shear angle." Further, it is assumed that *PQ* and *SR* are straight lines, and the length from their intersection O_ρ to *P* is the curvature radius ρ_0. In this paper $1/\rho_0$ is called the "equivalent curvature." If the radius of curvature of *PS* is r_0 and the center of curvature with the r_0 is O_r, $1/\rho_0$ and the curvature $1/r_0$ of *PS* have the geometric relationship expressed by equation (1).

$$\frac{1}{\rho_0} = \frac{1}{r_0} - \frac{d\psi_0}{dx_0} \tag{1}$$

The line segment before deformation corresponding to the deformed line segment *A'B'* is defined as *AB*. Assuming that the equivalent curvature radius of *AB* is ρ, the circumferential strain ε_x of *A'* is given by equation (2). *y* is the distance in the flange height direction after deformation. Assuming that the distance in the flange height direction before deformation is *Y*, the relationship between *y* and *Y* is given by equation (3). Assuming incompressibility, strain ε_y in the flange height direction (*y*-axis) and strain ε_z in the plate thickness direction (*z*-axis) are expressed by equation (4).

$$\varepsilon_x = \ln\left(\frac{\rho_0}{\rho}\right) = -\frac{2}{3}\ln\left(1 - \frac{3}{2}\frac{y}{\rho_0}\right) \tag{2}$$

$$y = \frac{2}{3}\rho_0\left\{1 - \left(1 - \frac{Y}{\rho_0}\right)^{\frac{3}{2}}\right\} \tag{3}$$

$$\varepsilon_y = \varepsilon_z = -\frac{\varepsilon_x}{2} \tag{4}$$

Furthermore, if the line segments in the *y* direction are kept straight before and after the deformation, the distribution of the shear angle ψ in the flange height direction is given by equation (5).

$$\psi = \frac{\rho_0}{\rho}\psi_0 \tag{5}$$

The circumferential stress σ_x and the shear stress τ are expressed by equations (6) and (7) assuming the total strain theory. The stress σ_y in the flange height direction and the stress σ_z in the plate thickness

direction are 0. The work-hardening characteristic of the steel sheet was expressed by equation (8). σ_{eq} is the equivalent stress. C is the strength coefficient, ε_0 is the initial strain and n^* is the work-hardening exponent, which are a constant determined by the material. From equation (8), it is possible to consider the influence of work hardening characteristics in this analysis. ε_{eq} is the equivalent plastic strain in the von Mises yield condition by equation (9).

$$\sigma_x = \sigma_{eq}\frac{\varepsilon_x}{\varepsilon_{eq}} \tag{6}$$

$$\tau = \frac{\sigma_{eq}}{3}\frac{\psi}{\varepsilon_{eq}} \tag{7}$$

$$\sigma_{eq} = C(\varepsilon_0 + \varepsilon_{eq})^{n^*} \tag{8}$$

$$\varepsilon_{eq} = \sqrt{\varepsilon_x^2 + \frac{\psi^2}{3}} \tag{9}$$

The bending moment M is expressed by equation (10). The shear force Q is expressed by equation (11). The relationship between the thickness of the flange after deformation t and the thickness of the flange before deformation T is expressed by equation (12).

$$M = \int_0^h \sigma_x t y \, dy \tag{10}$$

$$Q = \int_0^h \tau t \, dy \tag{11}$$

$$t = T\exp(\varepsilon_z) \equiv T\exp\left(-\frac{\varepsilon_x}{2}\right) \tag{12}$$

The equilibrium state of the moment regarding point P of the flange area element $PQ'R'S$ in Figure 1 is expressed by equation (13).

$$\frac{dM}{dx_0} + Q = 0 \tag{13}$$

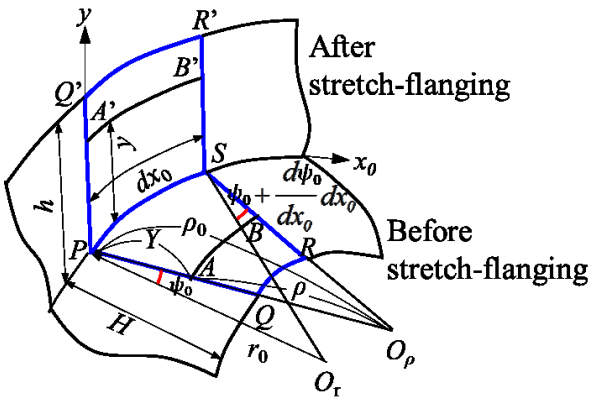

Figure 1. Configuration and symbols of the area element before and after deformation [4].

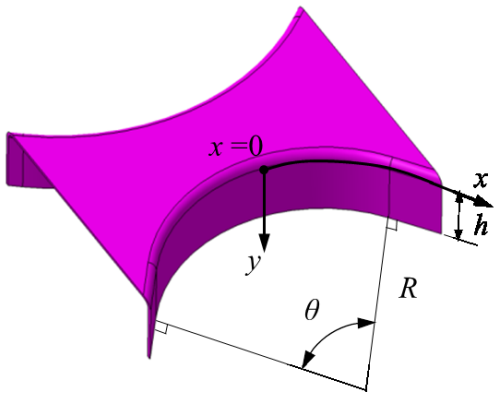

Figure 2. Shape of stretch-flanging.

3. Numerical method and results

3.1. Numerical method

In this study, the strain distribution in the circumferential direction at the flange edge was calculated using the numerical method in Chapter 2 and the stretch flangeability was evaluated. Table 1 shows the mechanical properties of steel sheets and the material parameters in equation (8) measured by the uniaxial tensile test. The part shape has a flat top surface and flange surfaces that comprise straight lines and circular arcs as shown in Figure 2. Corner radius R, shape angle θ, and flange height h were varied as shape variables. Corner radius R is the radius of curvature of the part, and it is a constant value inside circular arcs. The strain distribution was calculated by setting the corner radius R to 60mm, shape angle θ to 60 degrees, and flange height h to 18mm.

Calculation was performed by the finite difference method. The flange height h and the curvature radius ρ_0 are functions in the x-axis direction. The boundary condition, ψ_0=0, is adopted because of the symmetry at the center of the circular arc (x=0) in Figure 2. In addition, $1/\rho_0$=0, is adopted at the longitudinal end in the x-axis direction. The calculation procedure is shown as follows [4].

(1) $1/\rho_0$ is assumed at the center of the circular arc (x=0).
(2) As the calculation area, the flange height direction and the circumferential direction are divided by an arbitrary number of sections. The flange height direction was divided into 19 parts, and the circumferential direction was divided into 20 parts.
(3) ε_x at each point divided into Δy is calculated from equation (2), and σ_x and t are calculated from equations (6) and (12). Then, M is calculated from equation (10). From the boundary condition at the center of the circular arc (x=0), Q= 0, ψ_0=0.
(4) ψ_0 and M at x=Δx are calculated from equations (1) and (13) as the forward difference.

$$\psi_{02} = \psi_{01} + \left(\frac{1}{r_0} - \frac{1}{\rho_0}\right)\Delta x \tag{14}$$

$$M_2 = M_1 - Q\Delta x \tag{15}$$

Subscripts $(\ )_1$ and $(\ )_2$ indicate the variables of the previous position and the current position separated by Δx. $(\ )_1$ is a known variable. $1/\rho_{02}$ and Q_2 are calculated from equations (10) and (11) using M_2 and ψ_{02} is calculated from equations (14) and (15). Procedures (3) and (4) are repeated at each division point in the x direction to calculate $1/\rho_0$, Q, ε_x, σ_x and t in the circumferential direction.

(5) It is checked whether $1/\rho_0$ becomes equal to 0 at the edge. If it is not 0, $1/\rho_0$ in the center is corrected and procedures (1) to (4) are calculated again. Then, the calculation is repeated until the boundary condition at the edge is satisfied.

In order to investigate the accuracy of the strain distribution at the edge of the flange calculated from this method, FEA was performed by the dynamic explicit method on the model shape shown in Figure 2. The commercially available code LS-DYNA ver.971 R5.11 is used for FEA. The element type is a 4-node complete integral element, the number of integration points is 9 in the thickness direction, and the initial mesh size is 1.6mm.

In order to investigate the quantitative relationships between the strain at the edge and the shape variables, this calculation was performed under various shape conditions. For the range of the shape conditions, corner radius R was from 45 to 90 mm, shape angle θ was from 10 to 150 degrees, and flange height h was from 8 to 24 mm. The evaluation indicator was the circumferential strain ε_c at the center of the circular arc.

Table 1. Mechanical properties and parameters.

T / mm	YS / MPa	TS / MPa	El / %	C / MPa	ε_0	n*
1.6	411	602	32	969	0.005	0.178

3.2. Results

Figure 3 shows circumferential strain distribution ε_x at the flange edge calculated by uniform deformation theory and non-uniform deformation theory. The analysis result by non-uniform deformation theory considering the shear deformation shows that ε_x gradually decreases from the center of the circular arc to the straight end. On the other hand, ε_x was calculated by uniform deformation theory from equation (2). As a result, ε_x was a constant value inside a circular arc. Figure 4 shows shear angle ψ distribution at the flange edge calculated by non-uniform deformation theory. Shear angle ψ distribution shows the maximum value at the boundary between the circular arc and the straight end, hereafter called the "R end." Figure 5 shows the influence of work hardening exponent n^* on strain distribution. When n^* gradually increased from 0.17 to 0.30, from equation (8), it is possible to consider the influence of work hardening characteristics on the strain distribution in this method at the center of the circular arc is small. On the contrary, ε_x at the straight end is large. Figure 6 shows a comparison of ε_x in the analysis by the non-uniform deformation theory and the FEA. For each calculation result, ε_x at the center of the circular arc is almost the same value. Moreover, it is possible to qualitatively calculate the reduction of the ε_x from the center of the circular arc to the straight end.

We investigated the relationship between the designed variables (R, h, θ) of the parts and circumferential strain ε_c at the center of the circular arc. Figure 7 shows the relationship between ε_c and flange height h, and Figure 8 shows the relationship between ε_c and corner radius R. Their results were calculated assuming that shape angle θ is constant at 60 degrees. These results indicate that ε_c increased as flange height h increased, and ε_c decreased as corner radius R increased. Similarly, the relationship between ε_c and shape angle θ is shown in Figure 9. The results were calculated assuming that the corner radius R is constant at 60 mm. As a result, ε_c continuously increased as shape angle θ increased, and ε_c tended to be saturated when θ was further increased. It was also observed that the boundary condition at the edge could not be satisfied under the conditions of high ε_c in Figures 7, 8, and 9.

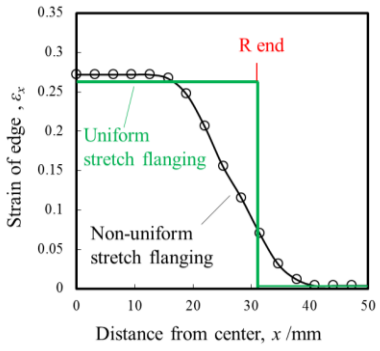

Figure 3. Circumferential strain ε_x and shear angle ψ calculated by uniform deformation theory.

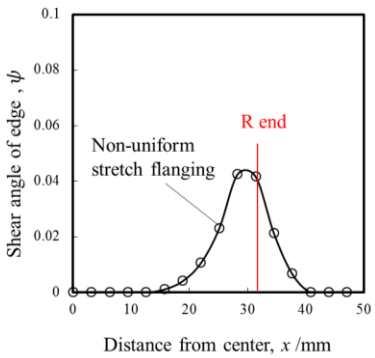

Figure 4. Shear angle distribution ψ calculated by non-uniform deformation theory.

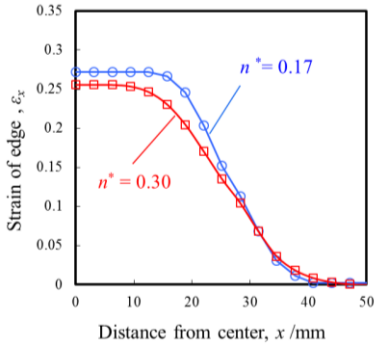

Figure 5. Influence of work hardening exponent n^* on circumferential strain distribution at the flange edge.

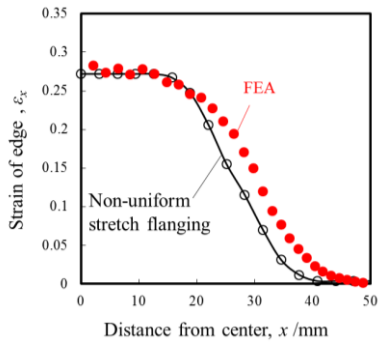

Figure 6. Comparison of analysis by non-uniform deformation theory and FEA in strain evaluation at the flange edge.

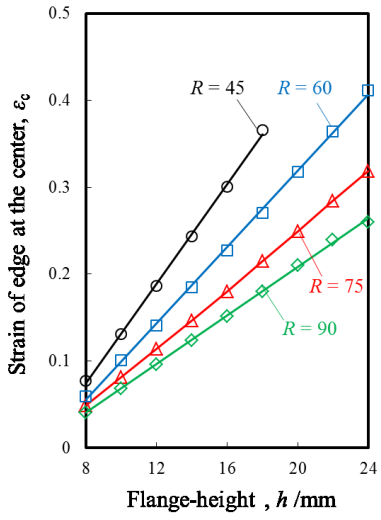

Figure 7. Relationship between strain of edge at center ε_c and flange-height h. (θ = 60 degrees)

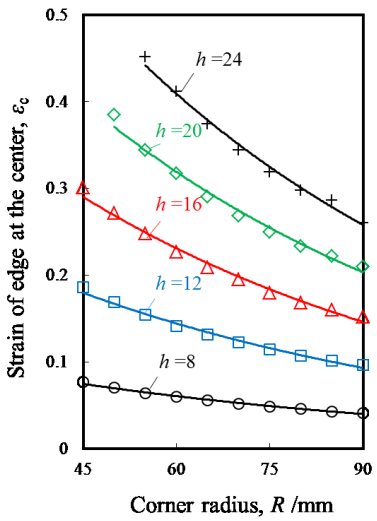

Figure 8. Relationship between strain of edge at center ε_c and corner radius R. (θ = 60 degrees)

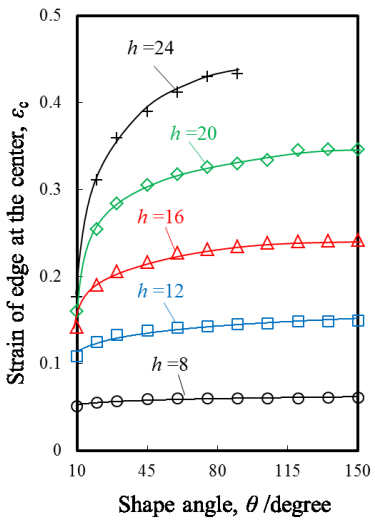

Figure 9. Relationship between strain of edge at center ε_c and shape angle θ. (R = 60 mm)

4. Discussion

The relationship between circumferential strain ε_c at the flange edge and designed variables (h, R, θ) is discussed as follows. Nagai revealed that it is necessary to lower the flange height h or increase the corner radius R in order to decrease ε_c [4]. Therefore, Figure 10 shows the relationship between ε_c and h/R. ε_c monotonically increases with h/R. This result shows that ε_c is uniquely determined irrespective of corner radius R. The reason for this is considered to be as follows. The part shape of this study has a circular arc and straight ends. The curvature of the flange decreases greatly near the R end. Therefore, bending moment M acting on the flange also decreases greatly in the circumferential direction. Figures 11 and 12 show bending moment M distribution and shear force Q distribution of the flange edge calculated by setting corner radius R to 60mm, shape angle θ to 60 degrees, and flange height h to 18mm. Shearing force Q acts on the flange to satisfy equation (11), and shear angle ψ occurs on the flange as shown in Figure 4. This shear angle ψ is maximum at the R end. Then shear angle ψ decreases from the R end to the center of the circular arc. As a result, $d\psi/dx$ becomes very small at the center of the circular arc, and $1/\rho$ gradually approaches $1/R$ from equation (1). In such a case, ε_c is almost proportional to h/R from equation (2).

Figure 13 shows the relationship between shape angle θ and the equivalent curvature $1/\rho_{0c}$ at the center of the circular arc. The equivalent curvature $1/\rho_{0c}$ also increases as shape angle θ increases. Therefore, ε_c continuously increased as shape angle θ increased. However, even if shape angle θ increases beyond a certain angle, the equivalent curvature $1/\rho_{0c}$ became saturated at a constant value. In such a case, a further increase in shape angle θ, reduces the increasing rate of ε_c. As described above, the influence of flange height h and corner radius R on ε_c is large, and the influence of shape angle θ is different depending on the size of the angle.

Figure 14 shows the part design method using non-uniform deformation theory in stretch-flanging analysis. Contour lines of ε_c are shown in Figure 14. Figure 14(a) shows ε_c under the condition with corner radius R and flange height h as variables. The results shown in Figure 14(a) were calculated assuming that the shape angle θ is constant at 60 degrees. Figure 14(b) shows ε_c under the condition with shape angle θ and flange height h as variables. The results shown in Figure 14(b) were calculated assuming that corner radius R is constant at 60 mm. In the range where ε_c is large in Figure 14, the risk of edge cracking is considered to be high. In addition to Figure 14, by setting critical strain ε_{cr} at which the flange edge fractures, it is possible to design a part shape that does not cause edge cracking. For

setting critical strain ε_{cr}, it is necessary to determine the value according to the type of steel and the processing conditions of the edge. Therefore, critical strain ε_{cr} was determined from the hole expansion ratio which is an index of stretch flangeability [5]. Regarding hole expansion ratios, the holes punched in specimens with 11%t clearance were expanded using a conical punch until a crack generated on the punched surface percolated across the entire material thickness, according to ISO16630 [6]. Hole expansion ratio λ and critical strain ε_{cr} are calculated from equations (16) and (17). Where d_0 is the initial hole diameter and d is the hole diameter after the hole expanding test.

$$\lambda = \frac{d - d_0}{d_0} \times 100 \tag{16}$$

$$\varepsilon_{cr} = \ln(1 + \frac{\lambda}{100}) \tag{17}$$

For example, if the hole expansion ratio of the test material is 55%, critical strain ε_{cr} is 0.43. In order to satisfy $\varepsilon_c < 0.43$ in Figure 14, flange height h may be designed to be lower than 21 mm at corner radius R = 50mm, or flange height h may be designed to be lower than 23 mm at shape angle θ = 90 degrees. According to this evaluation method, it is possible to design a shape that prevents edge cracking.

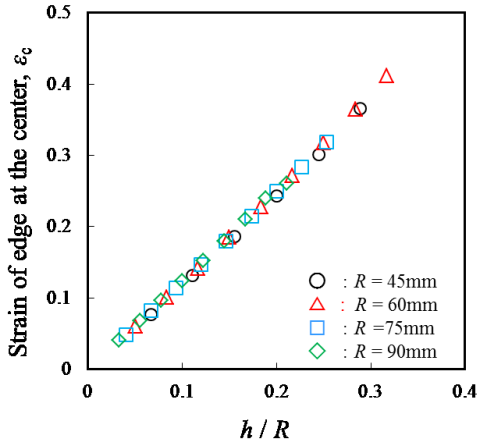

Figure 10 Strain ε_c vs. flange-height h/R for various corner radii. (θ = 60 degrees)

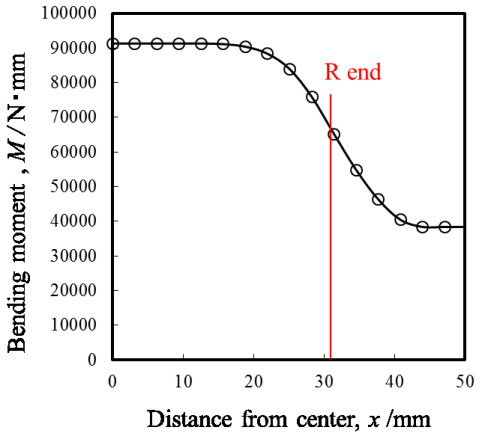

Figure 11 Bending moment M distribution calculated by non-uniform deformation theory.

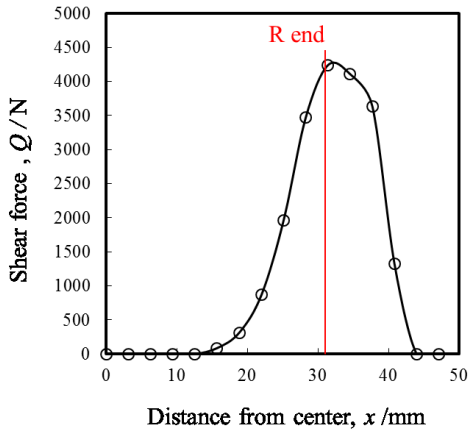

Figure 12 Shear force Q distribution calculated by non-uniform deformation theory.

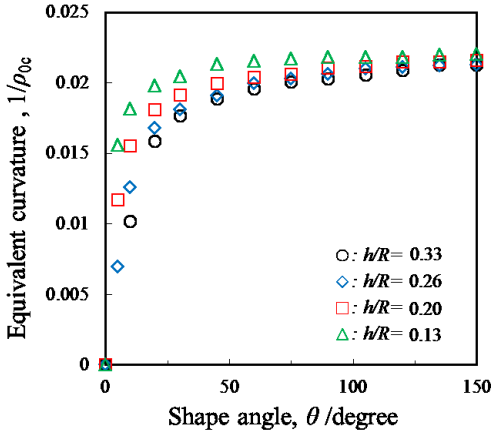

Figure 13 Equivalent curvature $1/\rho_{0c}$ vs. shape angle θ for various h/R. (R = 60 mm)

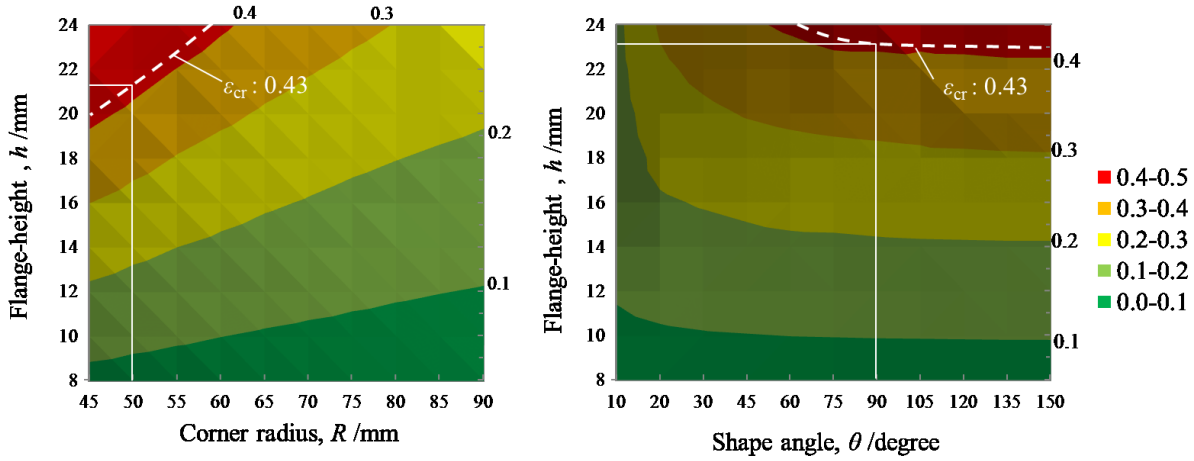

(a) Contour of strain ε_c according to flange height h and the corner radius R. (θ = 60 degrees)

(b) Contour of strain ε_c according to flange height h and the shape angle θ. (R = 60 mm)

Figure 14 Part design method using non-uniform deformation theory in stretch-flanging analysis.

5. Summary

In this study, the strain distribution at the flange edge in stretch-flanging was evaluated by using non-uniform deformation theory. The findings obtained from this study are shown below.

(1) The strains calculated by the finite difference method along the flange edge are comparable to those obtained by finite element analysis.
(2) In the part shape of this study, circumferential strain ε_c at the flange edge increased as corner radius R decreased or flange height h increased.
(3) The ε_c increased as shape angle θ increased. A further increase in θ, however, reduced the increasing rate of ε_c.
(4) We proposed a parts design method by stretch flanging analysis using non-uniform deformation theory.

Reference

[1] The Japan Sheet Metal Forming Research Group : Handbook of Ease or Difficulty in Press Forming 4th editions (2017) 10-12.
[2] J.Nitta, T.Yoshida, K.Hashimoto and Y.Kuriyama : "Development of the Practical Evaluation Test and a Study of Numerical Evaluations of Edge Fracture for Stretch Flange Formability of Sheet Metal Forming", International Deep Drawing Research Group IDDRG 2008 International Conference 16-18 (2008) 93-101.
[3] S.Hiwatashi and Y. Sakuma : "Stretch Flanging Limits of High-Strength Steels for Crashworthiness", Proceedings of Japan Society of Automotive Engineering 53 (2000) 20005112.
[4] Y.Nagai : "An Analysis of Non-Uniform Stretch Flanging of Sheet Metal", Journal of JSTP 24-266 (1983) 247-253.
[5] C.Butcher, A.David, M.Worswick : "Predictiong Failure during Sheared Edge Stretching Using a Damage-Based Model for the Shear-Affected Zone", International Journal of Materials and Manufacturing 6 (2013) 304-312.
[6] ISO 16630 : "Sheet and strip-Hole expanding test", (2009)